Organic & Biomolecular Chemistry

Cite this: *Org. Biomol. Chem.*, 2011, **9**, 5487

www.rsc.org/obc

PAPER

Trp-Trp pairs as β-hairpin stabilisers: Hydrogen-bonded *versus* non-hydrogen-bonded sites†

Clara M. Santiveri,[a] María Jesús Pérez de Vega,[b] Rosario González-Muñiz[b] and M. Angeles Jiménez*[a]

Received 7th March 2011, Accepted 5th May 2011
DOI: 10.1039/c1ob05353a

Trp–Trp pairs have emerged as a successful strategy for β-hairpin stabilization. Using loop 3 of Vammin as a template, we experimentally demonstrate that the contribution of Trp–Trp pairs to β-hairpin stability depends on β-sheet periodicity, that is, they are stabilising at non-hydrogen-bonded sites, but not at hydrogen-bonded positions.

Introduction

Hot spot mimicry to get bioactive peptides requires both structure stabilisation and conservation of biologically relevant residues. Loop regions, in particular, those belonging to β-hairpins, are often hot spots. Structurally, a β-hairpin consists of two hydrogen-bonded antiparallel β-strands connected by a loop region (Fig. 1). β-hairpins are classified according to the number of loop residues and hydrogen-bonds closing the loop.[1] The β-sheet region shows the periodicity characteristic of antiparallel β-sheets, in which two topologically different sites, hydrogen-bonded and non-hydrogen-bonded, alternate each other (Fig. 1). Side chains of residues belonging to each type of site point towards opposite sides of the β-sheet plane (Fig. 1). The two sites also differ in the geometrical relationships between the side chains of the facing residues. These features have to be taken into account for the rational design of β-hairpin forming peptides. Obviously, the residues to be conserved because of its key role in biological functionality can be located at any position. However, most tools available in our current "toolbox" for β-hairpin design work better for non-hydrogen-bonded than for hydrogen-bonded sites. For example, in agreement with statistical data on protein structures,[2–4] disulfide bonds have proven to be very suitable for stabilising β-hairpin structures at non-hydrogen-bonded sites, but not so well at hydrogen-bonded sites.[5] Trp–Trp pairs have also been shown to be excellent β-hairpin stabilisers at non-hydrogen-bonded sites.[6–16] In fact, the most stable linear β-hairpin peptides designed up to now, named Trpzip peptides,[7,11,13–14] contain one or two Trp–Trp pairs at non-hydrogen-bonded sites. Trp residues are also crucial for the stability of non-β-hairpin miniproteins, such as the Trp-cage,[17] and forms part of a recently identified C-terminal β-hairpin capping motif.[11–12,18] Statistical studies in proteins point out to a preference of Trp–Trp pairs at non-hydrogen-bonded sites relative to hydrogen-bonded sites, but they are not reliable because of the low abundance of Trp residues.[2–4] However, the single reported case of a Trp–Trp pair incorporated at a hydrogen-bonded site of a β-hairpin system led to β-hairpin destabilisation.[18] With all this in mind, we aimed to get further experimental data about whether β-hairpins are destabilised by Trp–Trp pairs at hydrogen-bonded sites. If so, peptide designers should avoid having them at hydrogen-bonded sites. On the contrary, if they were stabilising at least in certain cases, the β-hairpin design toolbox would count with an additional tool and so become more versatile.

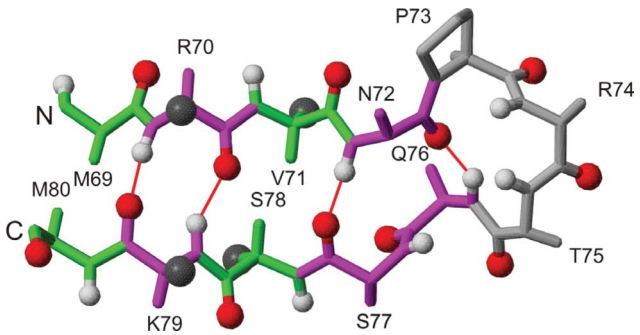

Fig. 1 Backbone structure of the loop 3 of Vammin in the crystalline structure (1WQ8), an antiparallel 4 : 6 β-hairpin with a non-Gly β-bulge formed by residues Q76 and S77. N- and C-termini are indicated. Residues are labelled at the H_α protons. Oxygen atoms are displayed as red spheres, and the proton atoms of NH groups as white spheres. Non-hydrogen-bonded sites are shown in green with the H_α protons pointing inwards, and hydrogen-bonded sites are in magenta with thin lines connecting the hydrogen-bonded CO and NH groups. Black spheres correspond to the side chain C_β carbons of facing residues in a hydrogen-bonded site (upwards) and in a non-hydrogen-bonded site (downwards). All the heavy atoms are shown for the proline side chain.

Results and Discussion

Peptide design

As a model system, we have taken the Vammin loop 3's skeleton (Fig. 1). Vammin is a member of the VEGF protein family. We

[a]*Instituto de Química Física Rocasolano, CSIC, Serrano 119, 28006, Madrid, Spain. E-mail: majimenez@iqfr.csic.es*
[b]*Instituto de Química Médica, CSIC, Juan de la Cierva 3, 28006, Madrid, Spain*

† Electronic supplementary information (ESI) available: Tables listing chemical shifts, distance and angle constraints used for structure calculation of peptide **W2W11**. See DOI: 10.1039/c1ob05353a

Table 1 ^{1}H chemical shifts (ppm) for the Trp side chains of peptides **W2W11** and **W3W10**[15] in aqueous solution at pH 5.5 and 5 °C

Peptide	Residue	$C_{\beta\beta'}H$	$C_{\delta1}H$	$C_{\varepsilon3}H$	$C_{\zeta3}H$	$C_{\eta2}H$	$C_{\zeta2}H$
W3W10	W3 edge	2.74, 2.19	6.87	5.35	6.42	6.86	7.19
	W10 face	3.30, 3.15	7.58	7.40	7.17	7.29	7.33
W2W11	W2	3.21, 3.21	7.25	7.57	7.13	7.21	7.49
	W11	3.29, 3.29	7.22	7.60	7.13	7.22	7.47
Random coil[a]	W	3.29, 3.27	7.27	7.65	7.18	7.25	7.50

[a] Random coil values were taken from Wishart *et al.*, 1995[24]

have previously reported[15] that the linear peptide encompassing residues 69–80 of Vammin (**Vam$_{69-80}$**; Fig. 2) is mainly a random coil, and that the replacement of the facing non-hydrogen-bonded residues V71 and S78 (Fig. 1) by a Trp–Trp pair leads to a peptide, denoted **W3W10** (Fig. 2), which adopts a well-defined native-like β-hairpin. To examine the stabilising capacity of a Trp–Trp pair located in a hydrogen-bonded site, we designed a new Vammin-derived peptide, **W2W11** (Fig. 2), by substituting the facing hydrogen-bonded residues R70 and K79 for a Trp–Trp pair (Fig. 1–2).[19]

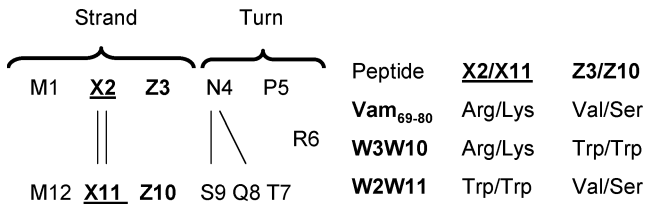

Fig. 2 Peptide sequences. β-sheet hydrogen-bonds are shown by lines. Turn and strand regions are indicated at the top. "X" and "Z" refer, respectively, to the hydrogen-bonded and non-hydrogen-bonded residues which are different in peptides **Vam$_{69-80}$**, **W3W10**, and **W2W11**. They are indicated at the right.

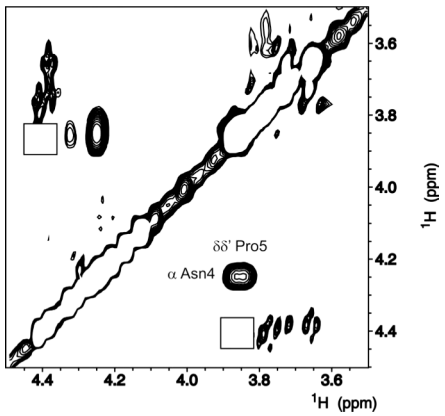

Fig. 3 Selected 2D NOESY spectral region of peptide **W2W11** in D_2O at pH 5.5 and 5 °C. The sequential NOE cross-peak between the $C_\alpha H$ proton of Asn4 and the $C_{\delta\delta'}H$ Pro5 is labelled on one side of the diagonal. A box indicates the position where the NOE cross-peak between the $C_\alpha H$ protons of Val3 and Ser10 would be observed, if present.

NMR structural analysis

NMR spectra of peptide **W2W11** were acquired in aqueous solution at pH 5.5 and 5 °C, the same conditions used in the NMR studies reported for peptides **Vam$_{69-80}$** and **W3W10**.[15] They showed a set of very minor signals attributed to the *cis* rotamer of the Asn–Pro bond,[20] as observed in peptides **Vam$_{69-80}$** and **W3W10**. The chemical shift difference between the Pro $^{13}C_\beta$ and $^{13}C_\gamma$ carbons[21] ($\delta_{C\beta} - \delta_{C\gamma}$ = 5.0 ppm; Table S1, ESI†) and the characteristic sequential NOEs observed between the H_α proton of N4 and the H_δ and $H_{\delta'}$ protons of P5 (Fig. 3) confirmed that the major species is the *trans* rotamer. From hereon in, we will refer only to the major *trans* species.

Trp side chains do not contact each other in peptide W2W11

In Trp–Trp pairs at non-hydrogen-bonded sites, the Trp side chains usually adopt an edge-to-face disposition.[16,22] In this orientation, the protons of the edge Trp side chain exhibit characteristic up-field chemical shifts,[23] as found for Trp3 in peptide **W3W10**[15] (Table 1). According to this, neither of the two Trp residues of peptide **W2W11** occupies an edge position, since the ^{1}H chemical shifts of both Trp residues are very close to random coil values (Table 1). Also, in contrast to peptide **W3W10** for which we found multiple NOEs between the side chain protons of the two Trp residues,[15] no NOE involving Trp side chains was detected in the case of peptide **W2W11**. The absence of Trp2–Trp11 NOEs could be explained by signal overlap as a consequence of the similitude of their chemical shifts. Thus, the absence of the edge-to-face arrangement does not discard that the Trp side chains might contribute to β-hairpin stability by another interacting way.

Peptide W2W11 does not fold into a β-hairpin structure

The strongest NMR evidence for a peptide adopting an ordered structure is the presence of non-sequential NOEs. Several of them are present in the NOESY spectra of peptide **W2W11** (Fig. 5). However, among them, we could not find any of the long-range NOEs characteristic of the expected β-hairpin (Fig. 1). In particular, we could not detect the NH W2–NH W11, and Hα V3–Hα S10 NOEs, even though, based on chemical shift values (Table S1, ESI†), they are far enough from the diagonal to be observable (Fig. 3). This indicates that peptide **W2W11** does not adopt the target β-hairpin, but some other ordered structure.

Further support of this result comes from the fact that, in contrast to peptide **W3W10**,[15] the pattern of chemical shift deviations observed for peptide **W2W11** (Fig. 4) does not conform to that expected for a β-hairpin (strand residues with negative $\Delta\delta_{C\alpha}$ values and positive $\Delta\delta_{C\alpha H}$, $\Delta\delta_{C\beta}$, and $\Delta\delta_{NH}$).[25–26]

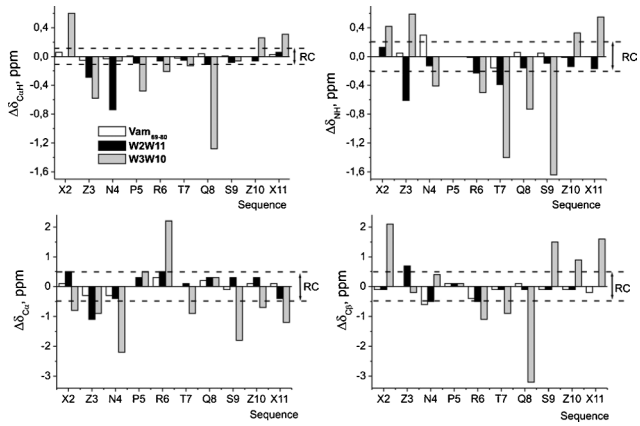

Fig. 4 Histograms showing the $\Delta\delta_{C\alpha H}$ ($\Delta\delta_{C\alpha H} = \delta_{C\alpha H}{}^{observed} - \delta_{C\alpha H}{}^{RC}$, ppm), $\Delta\delta_{C\alpha}$ ($\Delta\delta_{C\alpha} = \delta_{C\alpha}{}^{observed} - \delta_{C\alpha}{}^{RC}$, ppm), $\Delta\delta_{C\beta}$ ($\Delta\delta_{C\beta} = \delta_{C\beta}{}^{observed} - \delta_{C\beta}{}^{rRC}$, ppm) and $\Delta\delta_{NH}$ ($\Delta\delta_{NH} = \delta_{NH}{}^{observed} - \delta_{NH}{}^{RC}$, ppm) values as a function of sequence for peptides **Vam_{69-80}** (white bars), **W2W11** (black bars), and **W3W10** (grey bars) in aqueous solution at pH 5.5 and 5 °C. Dashed lines indicate the random coil (RC) ranges. Random coil values for $C_\alpha H$ protons and C_α and C_β carbons were taken from Wishart *et al.*, 1995.[24] $\Delta\delta_{NH}$ values were obtained by using the CSDb program (http://andersenlab.chem.washington.edu/CSDb/).[25] The $\Delta\delta_{C\alpha H}$, $\Delta\delta_{C\alpha}$ and $\Delta\delta_{C\beta}$ values of the Pro-preceding residue Asn4 were corrected for the Pro effect.[24] The N- and C-terminal residues are excluded because they are affected by their charged ends.

Peptide W2W11 adopts a non-random structure involving residues 2–8

The medium-range NOEs observed for peptide **W2W11** involve only residues 2–8 (Fig. 5 and Table 2). Interestingly, the only $\Delta\delta$ values which lie out of the random coil range belong to residues Val3, Asn4 and Thr7 within that region (Fig. 4). These results indicate that peptide W2W11 adopts some ordered structure in the region 2–8. Considering the small magnitude of the chemical shift deviations (Fig. 4), and the small number of medium-range NOEs (Table 2), that ordered structure is not highly populated

Table 2 Non-sequential NOEs observed for peptide **W2W11** in the 2D NOESY spectra recorded in aqueous solution at pH 5.5 and 5 °C

Residues i/j	Proton i	Proton j	NOE intensity
Trp 2/Asn 4	$C_{\varepsilon 1}H$	$C_\alpha H$	weak[a,b]
	$C_{\zeta 3}H$	$C_\alpha H$	weak[c]
	$C_{\zeta 3}H$	$C_\beta H$	weak[a,c]
	$C_{\zeta 2}H$	$C_\alpha H$	medium[a,c]
	$C_{\eta 2}H$	$C_\alpha H$	medium[a,c]
	$C_{\eta 2}H$	$C_\beta H$	weak[c]
Trp 2/Pro 5	$C_{\zeta 2}H$	$C_{\gamma\gamma'}H$	weak[c]
	$C_{\zeta 2}H$	$C_{\delta\delta'}H$	medium[a,c]
	$C_{\eta 2}H$	$C_{\delta\delta'}H$	weak[a,c]
Val 3/Pro 5	$C_\gamma H_3$	$C_\alpha H$	weak[c]
	$C_\gamma H_3$	$C_{\beta'}H$	weak[a,c]
Asn 4/Arg 6	$N_\delta H$	$C_\beta H$	weak[a,b]
	$N_\delta H$	$C_{\beta'}H$	weak[a,b]
Asn 4/Thr 7	$N_{\delta'}H$	$C_\gamma H_3$	weak[a,b]
	$C_{\beta'}H$	HN	weak[a,b]
Asn 4 or Arg 6/Gln 8	HN	$C_\beta H$	strong[a,b]
	HN	$C_{\beta'}H$	strong[a,b]
	HN	$C_{\gamma\gamma'}H$	strong[a,b]

[a] Observed in H_2O/D_2O 9 : 1 v/v. [b] NOEs involving amide protons are not observable in D_2O. [c] Observed in D_2O.

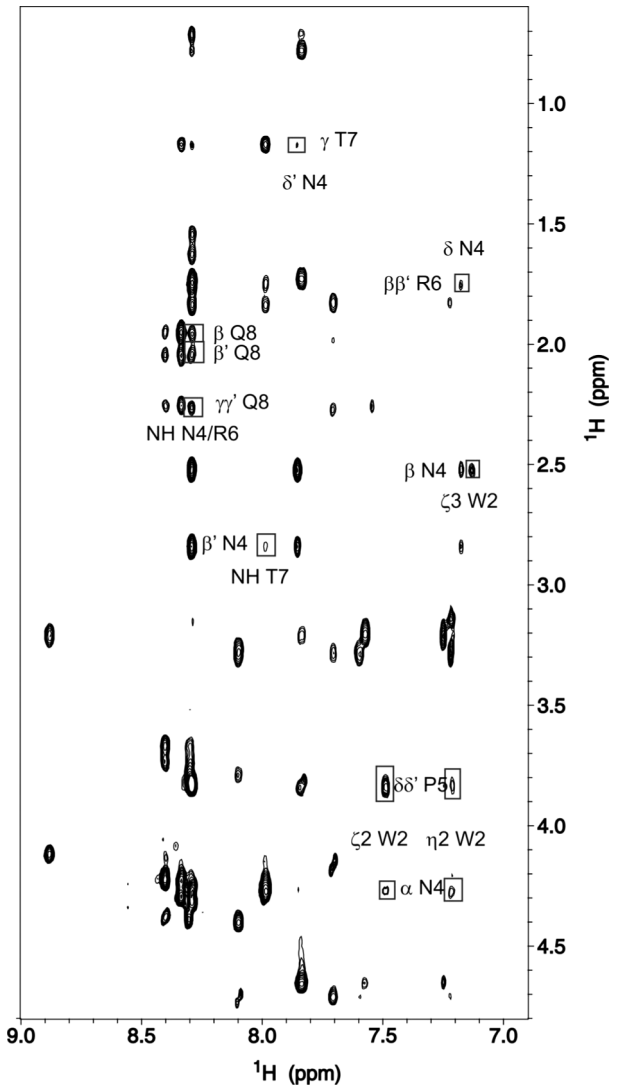

Fig. 5 Selected 2D NOESY spectral region of peptide **W2W11** in H_2O/D_2O 9 : 1 v/v at pH 5.5 and 5 °C. Non-sequential NOEs are boxed and labelled.

and coexists in equilibrium with random coil conformers. Because of this, structure calculation is not "truly" meaningful, but we performed it as a useful way to visualise and facilitate the qualitative analyses of the non-sequential NOEs as structural features of peptide **W2W1**. This model for the structure of peptide **W2W11** and that adopted by peptide **W3W10**[15] are displayed in Fig. 6.

The first noticeable feature is that the C-terminal region of peptide **W2W11** is mainly disordered, as qualitatively deduced from the absence of non-sequential NOEs and the chemical shift deviations being within the random coil range (Fig. 4). The side chain of the C-terminal Trp, for which we could not detect any non-sequential NOE, shows multiple conformations (Fig. 6a). In contrast, the N-terminal Trp side chain, which shows medium-range NOEs with Asn4 and Pro5 (Table 2), is relatively well-ordered. The observed Trp2–Asn4 NOEs are indicative of both side chains adopting a preferred orientation, which would contribute to fit the conformation of their common neighbour Val3, as seen in Fig. 6a. In addition, the side chain of Val is close

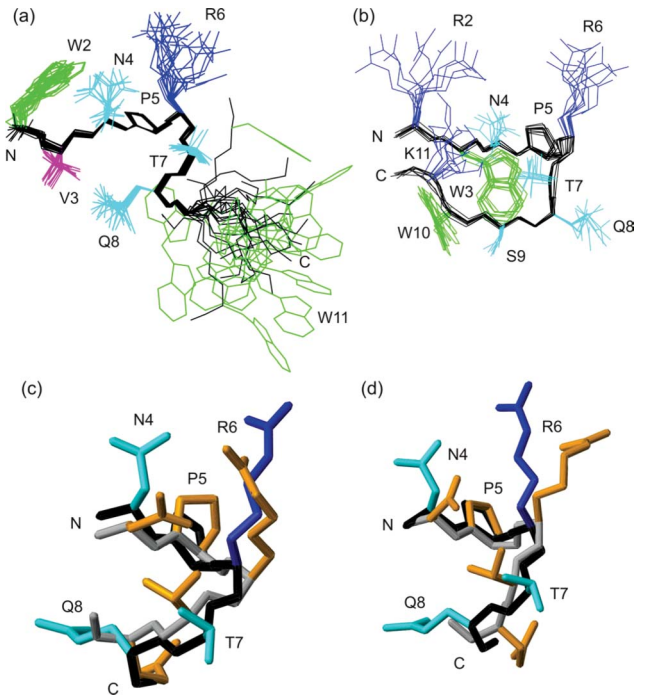

Fig. 6 (a) Model of the ordered structure adopted by peptide **W2W11**. Backbone and Pro side chain atoms are displayed in black, Trp side chains in green, Val in magenta, Asn, Thr, and Gln in cyan, and positively charged residues in blue. (b) NMR structure previously determined for peptide **W3W10**.[15] The same colour code as in panel (a) was employed. Ser side chain atoms are shown in cyan. (c & d) Residues 4–8 in the model structure of peptide **W2W11** superposed onto the loop 3 of Vammin (c; 1WQ8) and onto the same residues of peptide **W3W10** (d). Backbone and side chain atoms of peptide **W2W11** are coloured as in the top panel. For loop 3 of Vammin and for peptide **W3W10**, backbone atoms are shown in grey and side chains in orange. N- and C-termini are labelled in the four panels.

to the Pro ring ($C_\gamma H_3$ Val3 - $C_\alpha H/C_\beta H$ Pro5 NOEs; Table 2). Both facts would account for the chemical shift deviations of Val3 being out of the random coil range (Fig. 4). The anisotropy effect coming from the Trp2 indole ring also accounts for the Asn4 $\Delta\delta_{C\alpha H}$ value (Fig. 4). In fact, these anisotropy effects further indicate that the indole ring of Trp2 is in a relatively fixed position. In contrast, ^{1}H chemical shifts of the residues around Trp11, except for the $C_\beta H$ and $C_\gamma H$ protons of the following Met12 (Table S1, ESI†), do not show significant anisotropy effects. This fact suggests that the indole ring of Trp11 probably adopts multiple dispositions, as seen in Fig. 6a, so that most of its anisotropy effects on the neighboring protons compensate on the average.

Second, it is remarkable that some of the observed NOEs involving residues at the turn region, *i.e.* the amide side chain protons of Asn4 with the $C_{\beta\beta'}H$ protons of Arg6 and with the methyl group of Thr7 (Table 2 and Fig. 5), had also been found for the β-hairpin-forming peptide **W3W10**.[15] Indeed, residues 4–7 of the model structure calculated for peptide **W2W11** can be overlayed relatively well onto those residues in both the loop 3 of Vammin (Fig. 6c; RMSD for backbone atoms is 0.7 Å) and the structure of peptide **W3W10**[15] (Fig. 6d; RMSD for backbone atoms is 0.7 Å). This is also in agreement with the fact that both peptides share the pattern of chemical shifts at residues 5–7 (Fig. 4), but not the magnitude which is very small for peptide **W2W11**, and very significant for peptide **W3W10**. Concerning Gln8, its side chain protons are close to the amide protons of Asn4 and/or Arg6 in peptide **W2W11** (both amide protons have the same chemical shifts; and structure calculations suggest that Gln side chain can be close to both simultaneously), while Pro5–Gln8 NOEs were observed in peptide **W3W10**.[15] These different NOEs are probably a consequence of the arrangement of the Gln8 side chain in peptide **W2W11** differing from that of peptide **W3W10** (Fig. 6d).

Taking all this data together, we conclude that peptide **W2W11** adopts a local ordered structure spanning residues 2–8 (those for which non-sequential NOEs are found) and including a native-like turn at residues 4–7, which is in equilibrium with random coil structures.

Conclusions

Summarising, the incorporation of facing Trp–Trp pairs into a mainly disordered peptide, whose sequence comes from a protein β-hairpin (**Vam$_{69–80}$**; Fig. 1), leads to a peptide adopting a stable native-like β-hairpin if placed at a non-hydrogen-bonded site.[15] When placed at a hydrogen-bonded site, the Trp side chains do not interact with each other and no β-hairpin is formed. However, it provides some ordering at the N-terminal and turn regions (Fig. 6a). The side chains of the two Trp residues behave differently. That of the C-terminal Trp11 is completely disordered, whereas that of the N-terminal Trp2 shows a preferred orientation and some contacts to the side chains of Asn4 and Pro5. The sequence around the N-terminal Trp2 might represent a still unknown Trp-motif. Further work, out of the scope of this paper, would be required to confirm this hypothesis.

Differences in intrinsic amino acid β-sheet propensities might explain that peptide **W2W11** is more ordered than **Vam$_{69–80}$** since that of Trp is higher than those of Lys and Arg[27–29] (Fig. 2). Strikingly, based on intrinsic β-sheet tendencies, β-hairpin formation is less favorable in peptide **W3W10** than in peptide **W2W11** (Arg & Lys relative to Val & Ser;[27–29] Fig. 2). Thus, the distinct behavior of the Trp–Trp pair is very likely a consequence of the topological differences between both types of β-sheet sites (Fig. 1). In addition, the fact that Trp–Trp pairs do not favorably interact in hydrogen-bonded sites likely contributes to enhance the goodness of Trp–Trp pairs at non-hydrogen-bonded sites. In conclusion, the incorporation of facing Trp–Trp pairs at non-hydrogen-bonded sites is a well-established approach to stabilise β-hairpins, but we have experimentally shown here that this strategy cannot be applied at hydrogen-bonded sites. The generality of our results is supported by the only previous reported case of a Trp–Trp pair incorporated at a hydrogen-bonded site in another β-hairpin system[18] which, as in our case, was not stabilising. This finding is of high relevance for peptide and peptidomimetic design.

Experimental

Peptide synthesis

Peptide **W2W11** was synthesised by the solid phase method using Fmoc (fluorenyl-9-methyloxycarbonyl) protocols and purified by reverse-phase HPLC (RP-HPLC), up to more than 95% purity by CASLO Laboratory ApS (Lyngby, Denmark). RP-HPLC, linear

20–40% B/A gradient for 20 min, A: H_2O : CH_3CN (98 : 2, 0.05% TFA); B: H_2O : CH_3CN (10 : 90, 0.05% TFA); (t_R = 13.4 min; 98% purity). $[M + H]^{+calc}$ = 1523.78; $[M + H]^{+obs}$ = 1523.53. A list of ^1H, ^{13}C and ^{15}N chemical shifts is available in the ESI.†

NMR spectra

NMR samples were prepared by solving the lyophilised peptide (~1 mg) in H_2O/D_2O (9 : 1 ratio by volume; 0.5 mL) or in pure D_2O (0.5 mL). Peptide concentrations were about 1–2 mM. pH was adjusted to 5.5 by adding minimal amounts of NaOD or DCl, measured with a glass micro electrode and not corrected for isotope effects. The temperature of the NMR probe was calibrated using a methanol sample. Sodium 2,2-dimethyl-2-silapentane-5-sulfonate (DSS) was used as an internal reference.

The ^1H-NMR spectra were acquired on a Bruker AV-600 spectrometer operating at a proton frequency of 600.13 MHz and equipped with a cryoprobe. 1D spectra were acquired using 32 K data points, which were zero-filled to 64 K data points before performing the Fourier transformation. As previously reported,[15] 2D spectra, *i.e.*, phase-sensitive correlated spectroscopy (COSY), total correlated spectroscopy (TOCSY), and nuclear Overhauser enhancement spectroscopy (NOESY), were recorded by standard techniques using presaturation of the water signal and the time-proportional phase incrementation mode. NOESY mixing times were 150 ms and TOCSY spectra were acquired using 60 ms DIPSI2 with z filter spin-lock sequence. ^1H–^{13}C and ^1H–^{15}N heteronuclear single quantum coherence spectra (HSQC) were recorded at natural heteronuclear abundance using peptide samples in D_2O and in H_2O/D_2O 9 : 1 v/v, respectively. Acquisition data matrices were defined by 2048 × 512 (128 in the case of the ^1H–^{15}N HSQC spectrum) points in t_2 and t_1, respectively. Data were processed using the standard TOPSPIN program. The 2D data matrix was multiplied by either a square-sine-bell or a sine-bell window function with the corresponding shift optimised for every spectrum and zero-filled to a 2 K × 1 K (256 points in the ^1H–^{15}N HSQC) complex matrix prior to Fourier transformation. Baseline correction was applied in both dimensions. The 0 ppm ^{13}C and ^{15}N δ-values were obtained indirectly by multiplying the spectrometer frequency that corresponds to 0 ppm in the ^1H spectrum, assigned to internal DSS reference, by 0.25144953 and 0.101329118, respectively.

NMR assignment

^1H NMR signals of peptide **W2W11** were assigned by standard sequential assignment methods.[30] Then, the ^{13}C and ^{15}N resonances were straightforwardly assigned from the cross-correlations observed in the corresponding HSQC spectra between the proton and the bound carbon or nitrogen, respectively.

Structure calculation

Distance constraints were derived from the 150 ms mixing time 2D NOESY spectra recorded either in H_2O/D_2O 9 : 1 v/v or in D_2O. The NOE cross-peaks were integrated by using the automatic integration subroutine of the SPARKY program (T. D. Goddard and D. G. Kneller, Sparky 3, NMR Assignment Program, University of California, San Francisco, USA) and then calibrated and converted to upper limit distance constraints within the CYANA program.[31] After calibration, the intraresidual and the sequential distance contraints, for which contribution of random conformations can be large, were excluded. Then, structures were calculated using only the observed non-sequential distance constraints (A total of 18; Table S2, ESI†). The ϕ and ψ angle restraints for residues 2–4, 6 and 8 were derived from $^1H_\alpha$, $^{13}C_\alpha$ and $^{13}C_\beta$ chemical shifts using the TALOS program.[32] In the case of Thr7, the ranges of TALOS-derived ϕ and ψ angle values were very broad and therefore not incorporated as restraints in the structure calculation. The ϕ angles for residues 7 and 9–11 were restricted to the −180° to 0° range. Thus, 14 dihedral angles, 9 for φ angles and 5 for ψ, were restricted for structure calculation (Table S3, ESI†).

A total of 50 structures were calculated using the standard annealing strategy of the CYANA program.[31] The 20 structures with the lowest target function values were selected and energy-minimised (Maximum distance restraint violation is 0.1 Å; maximum torsion angle restraint violation 1.5°, and maximum van der Waals violation 0.04 Å). These structures were examined using the program MOLMOL.[33] Taking into account all residues, the pair wise root mean square deviations (RMSD) for these 20 structures are 2.4 ± 0.7 Å and 3.8 ± 0.7 Å for the backbone atoms, and for all heavy atoms, respectively. If only residues 2–8 are considered, the RMSD values go down to 0.3 ± 0.1 Å for the backbone atoms and to 1.5 ± 0.3 Å when side chain atoms are included.

Acknowledgements

We thank C. López and D. Pantoja-Uceda for technical assistance, and financial support from MICINN projects CTQ2008-00080/BQU and SAF2009-09323 and from CSIC Intramural projects 200580F0161 and 200580F0162.

Notes and references

1 B. L. Sibanda, T. L. Blundell and J. M. Thornton, *J. Mol. Biol.*, 1989, **206**, 759–777.
2 A. P. Cootes, P. M. Curmi, R. Cunningham, C. Donnelly and A. E. Torda, *Proteins*, 1998, **32**, 175–189.
3 E. G. Hutchinson, R. B. Sessions, J. M. Thornton and D. N. Woolfson, *Protein Sci.*, 1998, **7**, 2287–2300.
4 M. A. Wouters and P. M. Curmi, *Proteins*, 1995, **22**, 119–131.
5 C. M. Santiveri, E. Leon, M. Rico and M. A. Jimenez, *Chem.–Eur. J.*, 2008, **14**, 488–499.
6 S. J. Russell and A. G. Cochran, *J. Am. Chem. Soc.*, 2000, **122**, 12600–12601.
7 A. G. Cochran, N. J. Skelton and M. A. Starovasnik, *Proc. Natl. Acad. Sci. U. S. A.*, 2001, **98**, 5578–5583.
8 R. M. Fesinmeyer, F. M. Hudson and N. H. Andersen, *J. Am. Chem. Soc.*, 2004, **126**, 7238–7243.
9 R. Mahalakshmi, S. Raghothama and P. Balaram, *J. Am. Chem. Soc.*, 2006, **128**, 1125–1138.
10 M. Jager, M. Dendle, A. A. Fuller and J. W. Kelly, *Protein Sci.*, 2007, **16**, 2306–2313.
11 L. Eidenschink, B. L. Kier, K. N. Huggins and N. H. Andersen, *Proteins*, 2009, **75**, 308–322.
12 L. Eidenschink, E. Crabbe and N. H. Andersen, *Biopolymers*, 2009, **91**, 557–564.
13 T. Takekiyo, L. Wu, Y. Yoshimura, A. Shimizu and T. A. Keiderling, *Biochemistry*, 2009, **48**, 1543–1552.
14 L. Wu, D. McElheny, R. Huang and T. A. Keiderling, *Biochemistry*, 2009, **48**, 10362–10371.
15 Y. Mirassou, C. M. Santiveri, M. J. Perez de Vega, R. Gonzalez-Muniz and M. A. Jimenez, *ChemBioChem*, 2009, **10**, 902–910.
16 C. M. Santiveri and M. A. Jimenez, *Biopolymers*, 2010, **94**, 779–790.

17 J. W. Neidigh, R. M. Fesinmeyer and N. H. Andersen, *Nat. Struct. Biol.*, 2002, **9**, 425–430.
18 B. L. Kier, I. Shu, L. A. Eidenschink and N. H. Andersen, *Proc. Natl. Acad. Sci. U. S. A.*, 2010, **107**, 10466–10471.
19 Peptide **W2W11** was as water-soluble as $\mathbf{Vam}_{69\text{-}80}$, even though two positively charged residues, R70 and K79, were replaced by two large hydrophobic Trp residues.
20 Based on the intensities of TOCSY cross peaks corresponding to the Pro residue in the major and minor species, the *cis* percentage is about a 4%. Most linear Pro-containing peptides show about 5-10% *cis* X-Pro.
21 M. Schubert, D. Labudde, H. Oschkinat and P. Schmieder, *J. Biomol. NMR*, 2002, **24**, 149–154.
22 O. Guvench and C. L. Brooks, 3rd, *J. Am. Chem. Soc.*, 2005, **127**, 4668–4674.
23 N. H. Andersen, K. A. Olsen, R. M. Fesinmeyer, X. Tan, F. M. Hudson, L. A. Eidenschink and S. R. Farazi, *J. Am. Chem. Soc.*, 2006, **128**, 6101–6110.
24 D. S. Wishart, C. G. Bigam, A. Holm, R. S. Hodges and B. D. Sykes, *J. Biomol. NMR*, 1995, **5**, 67–81.
25 R. M. Fesinmeyer, F. M. Hudson, K. A. Olsen, G. W. White, A. Euser and N. H. Andersen, *J. Biomol. NMR*, 2005, **33**, 213–231.
26 C. M. Santiveri, M. Rico and M. A. Jimenez, *J. Biomol. NMR*, 2001, **19**, 331–345.
27 G. D. Fasman, in *Prediction of protein structure and the principles of protein conformation*, ed. G. D. Fasman, Plenum Press, New York, 1989, pp. 193–316.
28 C. K. Smith, J. M. Withka and L. Regan, *Biochemistry*, 1994, **33**, 5510–5517.
29 D. Pantoja-Uceda, C. M. Santiveri and M. A. Jiménez, *Methods Mol. Biol.*, 2006, **340**, 27–51.
30 K. Wuthrich, John Wiley & Sons, 1986, New York.
31 P. Guntert, C. Mumenthaler and K. Wuthrich, *J. Mol. Biol.*, 1997, **273**, 283–298.
32 G. Cornilescu, F. Delaglio and A. Bax, *J. Biomol. NMR*, 1999, **13**, 289–302.
33 R. Koradi, M. Billeter and K. Wuthrich, *J. Mol. Graphics*, 1996, **14**, 51–55, & 29–32.

